Nano Research 2016, 9(4): 963–973
DOI 10.1007/s12274-016-0984-2
Research Article

ISSN 1998-0124
CN 11-5974/O4

Large-area chemical vapor deposition-grown monolayer graphene-wrapped silver nanowires for broad-spectrum and robust antimicrobial coating

Chen Zhao[1,§], Bing Deng[2,§], Guanchu Chen[2], Bo Lei[2], Hong Hua[1], Hailin Peng[2] (✉), and Zhimin Yan[1] (✉)

[1] *Department of Oral Medicine, Peking University School of Stomatology, Beijing 100081, China*
[2] *Center for Nanochemistry, Beijing Science and Engineering Center for Nanocarbons, Beijing National Laboratory for Molecular Sciences (BNLMS), College of Chemistry and Molecular Engineering, Peking University, Beijing 100871, China*
[§] *These authors contributed equally to this work.*

Received: 14 November 2015
Revised: 9 December 2015
Accepted: 18 December 2015

KEYWORDS
graphene,
silver nanowires,
antimicrobial,
chemical vapor deposition (CVD),
electrochemical corrosion

ABSTRACT

New types of antimicrobial systems are urgently needed owing to the emergence of pathogenic microbial strains that gain resistance to antibiotics commonly used in daily life and medical care. In this study, we developed for the first time a broad-spectrum and robust antimicrobial thin film coating based on large-area chemical vapor deposition (CVD)-grown graphene-wrapped silver nanowires (AgNWs). The antimicrobial graphene/AgNW hybrid coating can be applied on commercial flexible transparent ethylene vinyl acetate/ polyethylene terephthalate (EVA/PET) plastic films by a full roll-to-roll process. The graphene/AgNW hybrid coating showed broad-spectrum antimicrobial activity against Gram-negative (*Escherichia coli*) and Gram-positive bacteria (*Staphylococcus aureus*), and fungi (*Candida albicans*). This effect was attributed to a weaker microbial attachment to the ultra-smooth graphene film and the sterilization capacity of Ag^+, which is sustainably released from the AgNWs and presumably enhanced by the electrochemical corrosion of AgNWs. Moreover, the robust antimicrobial activity of the graphene/AgNW coating was reinforced by AgNW encapsulation by graphene. Furthermore, the antimicrobial efficiency could be enhanced to ~100% by water electrolysis by using the conductive graphene/AgNW coating as a cathode. We developed a transparent and flexible antimicrobial cover made of graphene/AgNW/EVA/PET and an antimicrobial denture coated by graphene/AgNW, to show the potential applications of the antimicrobial materials.

Antimicrobial agents are widely used in daily life to treat and prevent many infectious diseases. Coatings with antimicrobial agents that can kill harmful microbes on contact are highly recommended for personal

Address correspondence to Zhimin Yan, yzhimin@gmail.com; Hailin Peng, hlpeng@pku.edu.cn

smartphones and tablets, automated teller machine (ATM), self-service kiosks used in hospitals, retail display fixtures, and other public facilities [1–2]. A variety of antimicrobials that prevent the attachment and proliferation of pathogenic microorganisms have been developed [3–4]. However, because microbes continuously develop resistance against most classes of antimicrobials, new classes of antimicrobials are urgently needed [5–7].

Emerging nanomaterials such as silver nanoparticles [8–11], silver nanowires [12–15], vanadium pentoxide (V_2O_5) nanowires [16], carbon nanotubes [17–18], and graphene [19–23] have already shown promising antimicrobial activity. As a natural antimicrobial material, silver exhibits broad-spectrum antimicrobial activity toward many pathogenic bacteria, fungi, and viruses [24]. In comparison with bulk silver, nanostructured silver with a high specific surface area, including colloid silver nanoparticles, showed significant improvement in antimicrobial activity, owing to specific effects such as strong adsorption at the microbial surface and enhanced silver ion (Ag^+) release [24–26]. The release of Ag^+ driven by its oxidative dissolution is considered to be the main mechanism of the antimicrobial activity of silver [27–28]. Indeed, silver nitrate and sulfadiazine containing Ag^+ are currently used in hospitals as broad-spectrum antimicrobial agents because of low toxicity. Nevertheless, Ag^+ is a cation that easily forms highly insoluble precipitates, such as Ag_2S [29] and AgCl [30], which result in a significant reduction of its antimicrobial capacity. Recently, graphene-based nanomaterials, including graphene oxide (GO) and reduced graphene oxide (rGO) nanosheets, showed effective inhibition of the growth of *Escherichia coli* through severe graphene insertion [19–21], formation of pores in the bacterial cell wall [23], or destructive lipid extraction [22]. In addition, the assembly of GO or rGO powder with colloid silver nanoparticles was reported to enhance the overall antibacterial activity, and even to confer special features such as controlled durative slow-release of Ag^+ ions [31–34]. However, the intrinsic antimicrobial activities of the graphene film, grown by the chemical vapor deposition (CVD) method, and its hybrid with silver nanostructures are still unclear [35–36].

On the other hand, the hybrid thin film of large-area monolayer graphene-covered silver nanowires (AgNWs) is a promising flexible transparent conductive film [37] for potential applications in displays [38], electrochromic smart windows [39], touchscreens, and healthcare-related wearable devices, among others, where the attachment and proliferation of pathogenic microorganisms remains a major safety issue. Hence, functionalizing those films with antimicrobial activity may significantly enhance the reliability and safety of the corresponding device's applications. For example, a nanostructured hybrid film of GO and AgNW has been reported as a transparent conductive film with antibacterial activity [33]. However, the antimicrobial activity of large-area CVD-grown graphene wrapped AgNW films, which show better optoelectronic properties than those of GO and AgNW hybrid films [33, 39], has never been reported.

Here, we demonstrated for the first time that a thin coating based on large-area CVD-grown monolayer graphene-wrapped AgNW networks exhibit efficient antimicrobial properties. The CVD-graphene/AgNW hybrid film showed broad spectrum and robust antimicrobial activity against various microorganisms, including Gram-negative (*E. coli*) and Gram-positive bacteria (*Staphylococcus aureus*), and fungi (*Candida albicans*). Moreover, based on the good electrical conductivity of the graphene/AgNW hybrid film, the antimicrobial efficiency could be enhanced to ~100% by water electrolysis by using the hybrid film as a transparent electrode.

A scheme of the structure and antimicrobial activity of the graphene thin film covered by AgNWs is shown in Fig. 1(a). The AgNW networks were partially embedded into the plastic substrate and fully encapsulated by large-area CVD-grown monolayer graphene film. The plastic substrate used in this work was a commercial flexible transparent plastic film made by ethylene vinyl acetate/polyethylene terephthalate (EVA/PET) bilayer polymer. Large-area monolayer graphene film was grown by low-pressure CVD on copper foil. The detailed fabrication process of graphene/AgNW hybrid film is described in the experimental section and illustrated in Fig. S1 in the Electronic Supplementary Material (ESM). Briefly, AgNWs were spin-coated onto the EVA/PET plastic

substrate and subsequently hot-laminated with graphene/Cu to form Cu/graphene/AgNW/EVA/PET stacked film. The graphene/AgNW/EVA/PET hybrid film was then obtained by removing the Cu foil with electrochemical bubbling delamination [39]. The microstructure of the hybrid film was first characterized by optical microscopy (OM) and afterwards by scanning electron microscopy (SEM), shown in Figs. 1(b) and 1(c), respectively. A network of AgNWs formed by an overlay of individual nanowires, which was fully covered by a monolayer graphene film, enabled the hybrid film to be electrically conductive. Note that the CVD-grown graphene usually exhibits a polycrystalline film with several micrometers to a few tens of micrometers, and thus contains a high density of grain boundaries and point defects [40–41], which may open up avenues for the corrosion of underlying AgNWs and diffusion of the released Ag^+. Moreover, some graphene cracks formed during the graphene transfer process, as indicated by red arrows in Fig. 1(c), also contribute to the release of Ag^+. The corresponding OM and SEM characterization of EVA/PET, graphene/EVA/PET, and AgNW/EVA/PET is shown in Fig. S2 in the ESM.

As obtained, graphene/AgNW/EVA/PET flexible film showed high transparency in a broad wavelength range from 320 to 2,000 nm of the UV-vis-NIR spectrum, depicted in Fig. 1(d). The absorption peak at ~380 nm was assigned to the AgNWs, which accounts for the transverse plasmon mode of AgNWs [42]. The inset of Fig. 1(d) exhibits a roll of flexible graphene/AgNW/EVA/PET film produced by a full roll-to-roll process [39], showing its potential in low-cost mass production of thin films with antimicrobial coating. The remarkable transparent and flexible nature of the hybrid thin film enables it to be easily fabricated as an antimicrobial

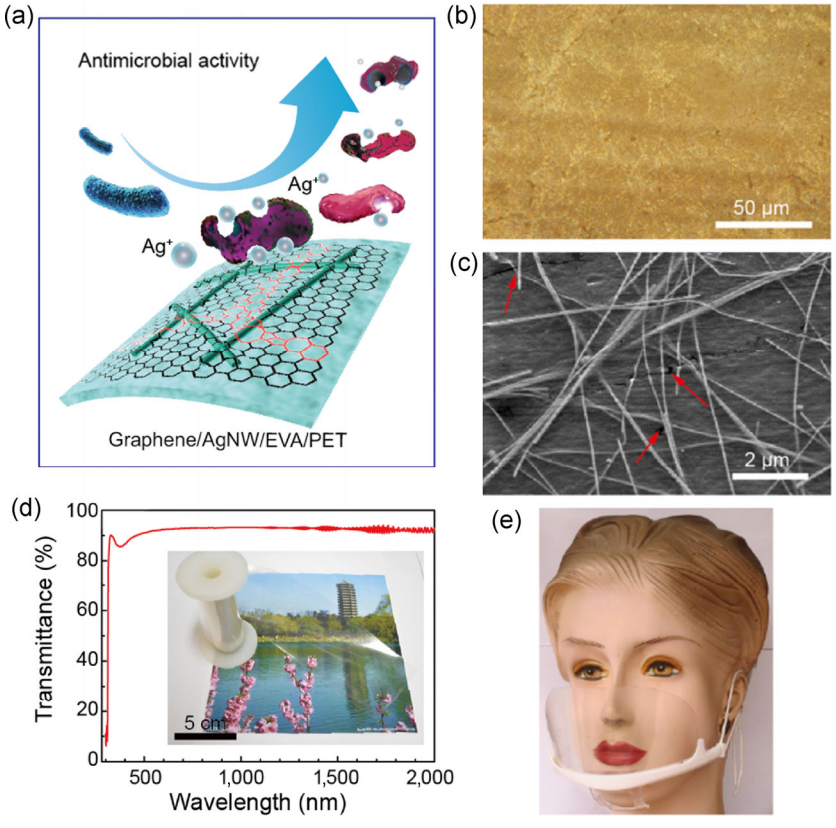

Figure 1 Structure and characterization of the CVD-grown graphene-wrapped silver nanowire hybrid film. (a) Scheme and mechanism of the antimicrobial activity of graphene-wrapped silver nanowire film. (b) OM image of the graphene/AgNW/ EVA/PET film. (c) SEM image of the graphene/AgNW/EVA/PET film, showing that AgNWs form a connected network completely covered by a monolayer of graphene film. Red arrows indicate cracks in the graphene film. (d) UV-vis-NIR spectrum of the graphene/AgNW/EVA/PET film, showing high transparency. The inset shows a photograph of a roll of transparent graphene/AgNW/EVA/PET film. (e) Photograph of a flexible and transparent antimicrobial cover made of the hybrid film.

mask, as it can be seen in Fig. 1(e).

The antimicrobial activity of the graphene/AgNW/EVA/PET hybrid film was carefully evaluated. *C. albicans* SC5314 was chosen as a microorganism model since it is the most prevalent fungal pathogen in humans, causing a wide range of diseases from superficial mucosal infections to deep-seated systemic invasions. As shown in Fig. 2(a), the number of colony forming units (CFU) of *C. albicans* on EVA/PET film was significantly higher than that on AgNW/EVA/PET, graphene/EVA/PET, and graphene/AgNW/EVA/PET films, which was evidenced by confocal laser scanning microscopy (CLSM) in Figs. 2(c)–2(f). The graphene/AgNW/EVA/PET hybrid film exhibited the lowest CFU counts, indicating that graphene/AgNW surface was effective at preventing microbial attachment.

In fact, microbial adhesion to biomaterial surfaces is the crucial step in biofilm formation and subsequent biomaterial-associated infections [43]. The control of microbial adhesion is essential to avoid infections, which is usually determined by both microbial characteristics and physicochemical properties of the material surface. From the material surface point of view, surface roughness, wettability, and chemistry influences bacterial adhesion [43]. Generally, rough surfaces harbor more microbes than smooth surfaces [44–45], whereas hydrophilic materials are more resistant to microbial attachment than hydrophobic materials [46–47]. As a unique two-dimensional atomic crystal made by a flat monolayer of sp^2-hybridized carbon atoms, graphene is chemically inert and ultrasmooth at the atomic level [48]. In addition, graphene

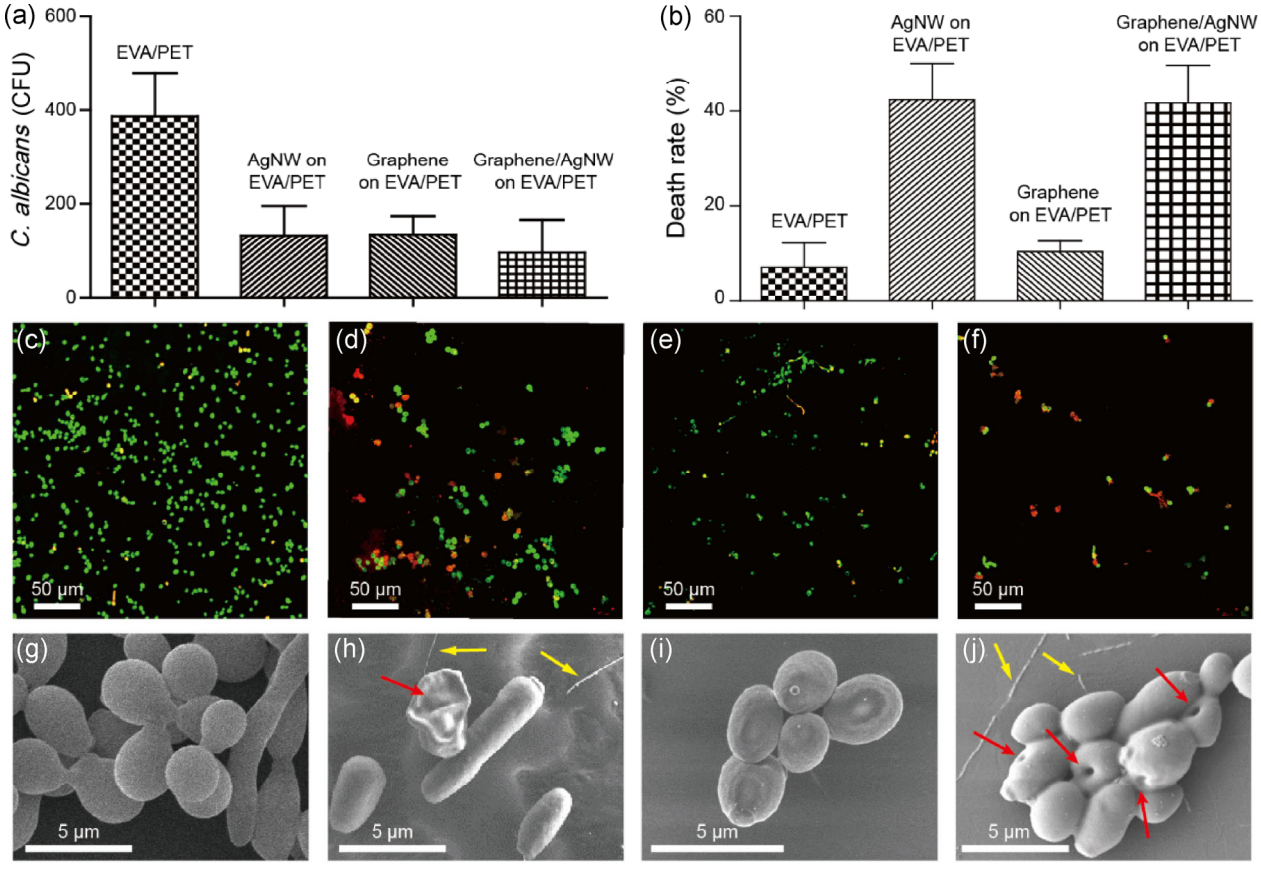

Figure 2 Antimicrobial activity of the graphene/AgNW hybrid film against *C. albicans*. CFU (a) and death rate (b) on EVA/PET, AgNW/EVA/PET, graphene/EVA/PET, and graphene/AgNW/EVA/PET films. The number of *Candida* cells shows that graphene coverage significantly decreases the attachment of microorganisms, whereas the death rate shows that the antimicrobial activity is mainly originated in the AgNWs. (c)–(f) CLSM of *C. albicans* on EVA/PET (c), AgNW/EVA/PET (d), graphene/EVA/PET (e), and graphene/AgNW/EVA/PET (f). Live cells are stained in green; dead cells are stained in red. (g)–(j) The equivalent SEM images of *C. albicans* on EVA/PET (g), AgNW/EVA/PET (h), graphene/EVA/PET (i), and graphene/ AgNW/EVA/PET films (j). Red arrows indicate the concave structure or collapse of dead cells and yellow arrows indicate AgNWs.

was reported to exhibit a moderately hydrophobic behavior with a contact angle (CA) of about 90°–95° [49]. Thus, graphene coverage significantly enhanced the smoothness and reduced the hydrophobicity of EVA/PET plastic substrate (~106°) to some extent, as indicated by contact angle measurements shown in Fig. S4 in the ESM. Both effects lead to a weaker microbial adhesion on the surface of the graphene-covered film.

Remarkably, the death rates of *C. albicans* on graphene/AgNW/EVA/PET and AgNW/EVA/PET films were over 4-fold higher than on the EVA/PET film, whereas graphene/EVA/PET film did not exhibit antimicrobial efficiency, as shown in Fig. 2(b). SEM imaging was used to further examine morphological changes in *C. albicans* on EVA/PET, AgNW/EVA/PET, graphene/EVA/PET, and graphene/AgNW/EVA/PET films shown in Figs. 2(g) and 2(j). The cell membrane of *C. albicans* remained intact on EVA/PET and graphene/EVA/PET films, as it can be observed in Figs. 2(g)–2(i). However, the membrane collapsed or was even perforated in the groups containing AgNWs, as an evidence of the crucial effect of AgNWs for antimicrobial efficiency evidenced in Fig. 2(h)–2(j). Thus, we can conclude that AgNWs account for the antimicrobial activity of the graphene/AgNW hybrid film, whereas the outer graphene layer played a role in reducing the attachment of microbes to the surface.

The antimicrobial mechanism of the AgNW/EVA/PET film can be attributed to the release of Ag^+ through the oxidation of Ag^0 by atmospheric oxygen dissolved in the water [14, 28]. Compared with the AgNW/EVA/PET film, the graphene/AgNW/EVA/PET film with a similar AgNW density exposed less area of silver to the microbial culture solution but exhibited almost the same antimicrobial capacity. This phenomenon can be explained by the electrochemical corrosion of silver. It has been reported that wet corrosion of a copper foil covered by graphene can be promoted due to electrochemical reactions [50]. Actually, since uncovered AgNWs are in direct contact with conductive graphene, a (−) Ag/electrolyte/graphene (+) primary battery might be formed when the graphene/AgNW hybrid film is placed into the electrolyte. Considering that the electrode potential of Ag (+0.7996V) is much smaller than that of graphene (+2.5V) [51−52], AgNWs would always work as the active anode and graphene as an inert cathode, which significantly enhance the corrosion of AgNW releasing Ag^+. The release of Ag^+ was confirmed by measuring the content of silver element by Inductively Coupled Plasma-Atomic Emission Spectrometer (ICP-AES), as shown in the experimental section. When graphene/AgNW/EVA/PET film was placed into acid solutions, the electrochemical corrosion type was hydrogen evolution

$$\text{Anode (AgNW)} \quad 2Ag - 2e^- = 2Ag^+ \quad (1)$$

$$\text{Cathode (graphene)} \quad 2H^+ + 2e^- = H_2 \quad (2)$$

Otherwise, oxygen reduction dominated the corrosion process when the hybrid film contacted with neutral or basic solutions

$$\text{Anode (AgNW)} \quad 4Ag - 4e^- = 4Ag^+ \quad (3)$$

$$\text{Cathode (graphene)} \quad 2H_2O + O_2 + 4e^- = 4OH^- \quad (4)$$

Afterwards, we evaluated the broad-spectrum antimicrobial activity of the graphene/AgNW/EVA/PET hybrid film. Besides the *C. albicans* evaluation mentioned above, the antimicrobial activities against the Gram-negative bacteria *E. coli* and the Gram-positive *S. aureus* were also tested. We found that graphene/AgNW/EVA/PET film exhibited efficient antimicrobial activity against both *E. coli* and *S. aureus,* as it can be inferred from Fig. 3. Both types of bacteria remained alive and intact on the surface of EVA/PET, as evidenced in Figs. S3(b) and S3(d) in the ESM. In contrast, the contact with the surface of the graphene/AgNW/EVA/PET film led to the development of holes in the cell membranes and subsequent collapse and death of both *E. coli* and *S. aureus*, as observed in Figs. 3(a)–3(b) and 3(d)–3(e). The antimicrobial efficiency of graphene/AgNW/EVA/PET film against bacteria is slightly reduced compared to *C. albicans*, even though approximately two times higher than that of EVA/PET plastic substrate without graphene/AgNW coating, as shown in Figs. 3(c) and 3(f). This broad spectrum of antimicrobial capacity makes the graphene/AgNW/EVA/PET hybrid film highly promising for practical applications [53].

Surprisingly, the monolayer graphene coverage did not reduce the antimicrobial activity of underlying AgNWs. On the contrary, the graphene coverage enables unprecedented advantages for robust antimicrobial

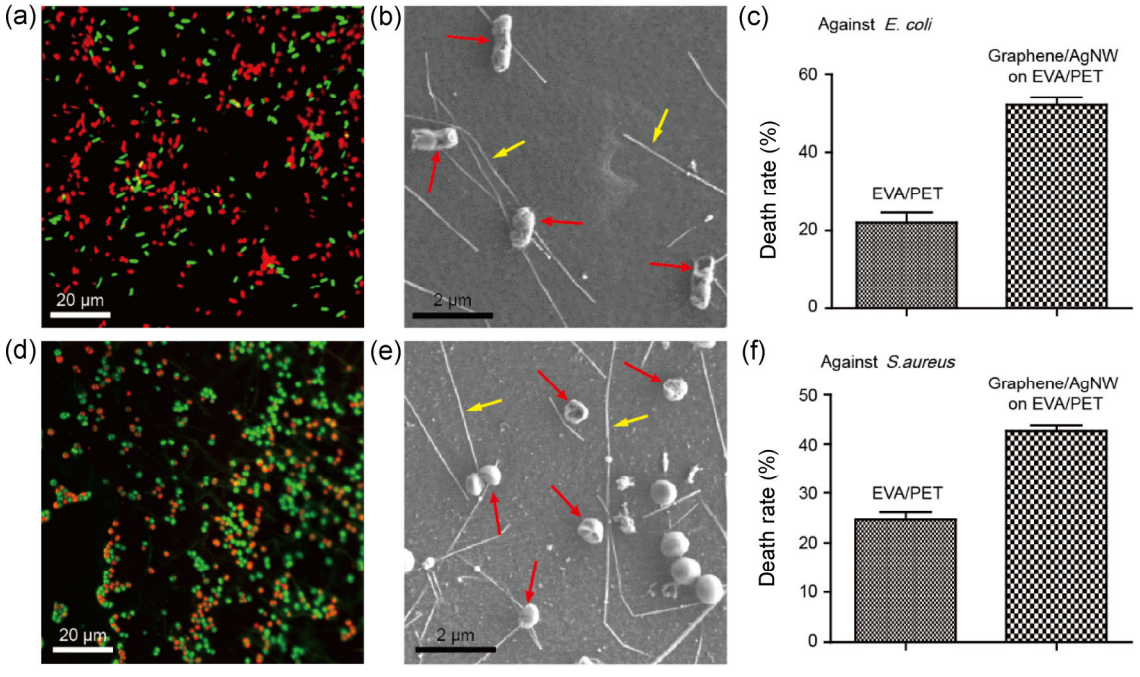

Figure 3 Antibacterial activity of the graphene/AgNW hybrid film against *E. coli* and *S. aureus*. (a) and (b) CLSM and SEM images of a graphene/AgNW/EVA/PET film against Gram-negative bacteria *E. coli*. (c) Death rate of *E. coli* from the CLSM image. (d) and (e) CLSM and SEM image of graphene/AgNW/EVA/PET film against Gram-positive bacteria *S. aureus*. (f) Death rate of *S. aureus* from the CLSM image. In the CLSM images, live cells are stained in green, whereas dead cells are stained in red. Red arrows indicate concave or collapsed dead cells, whereas yellow arrows indicate AgNWs in the SEM images.

activity of AgNWs, which is relevant for practical applications. As mentioned above, silver nanostructures are susceptible to many anions by forming extremely insoluble precipitates such as Ag_2S [29] and AgCl [30], which significantly suppress the release of Ag^+. On the other hand, chemically inert graphene can be used for corrosion-inhibiting coating for metallic nanostructures [54]. As shown in Fig. 4(a), the fully covered graphene/AgNW/EVA/PET can bear the sulfurization of underlying AgNWs in Na_2S solution with little degradation of antimicrobial activity against *C. albicans*. SEM images in Fig. 4(b) clearly show that AgNWs without graphene coverage were corroded severely until broken, whereas in Fig. 4(c) is shown that the shape of nanowires in graphene/AgNW/EVA/PET film remained intact under the attack of aqueous Na_2S. Moreover, the electrochemical corrosion of underlying AgNWs also enabled the sustained release of Ag^+ from the grain boundaries, and point defects of CVD-grown graphene film for robust antimicrobial activity, which greatly expanded the potential practical applications [55].

Another significant concern of nanomaterial-based antimicrobial systems is the toxicity issues for humans and the environment. Nanomaterials such as colloid nanoparticles and nanowires can be easily released into the environment owing to their ultra-small size and high surface reaction activity [26]. The rising concentration of silver as an environmental pollutant also increases the chance of exposure in humans [56]. Usually, owing to their weak adhesive force on the substrate, pre-coated AgNWs do not adhere and can be easily removed from the substrate under moderate friction forces or ultrasonic elution, as shown in Fig. 4(e). Remarkably, as Fig. 4(d) shows, the coated graphene/AgNW/EVA/PET film exhibited a constant antimicrobial activity against *C. albicans* even after long-time ultrasonic elution. We believe that the full encapsulation of AgNWs between graphene and the EVA supporting layer significantly enhanced the adhesion of AgNWs to the substrate, which made it more resistant to repeated ultrasonic elutions, significantly higher than the uncovered AgNW sample, as evidenced in Fig. 4(f).

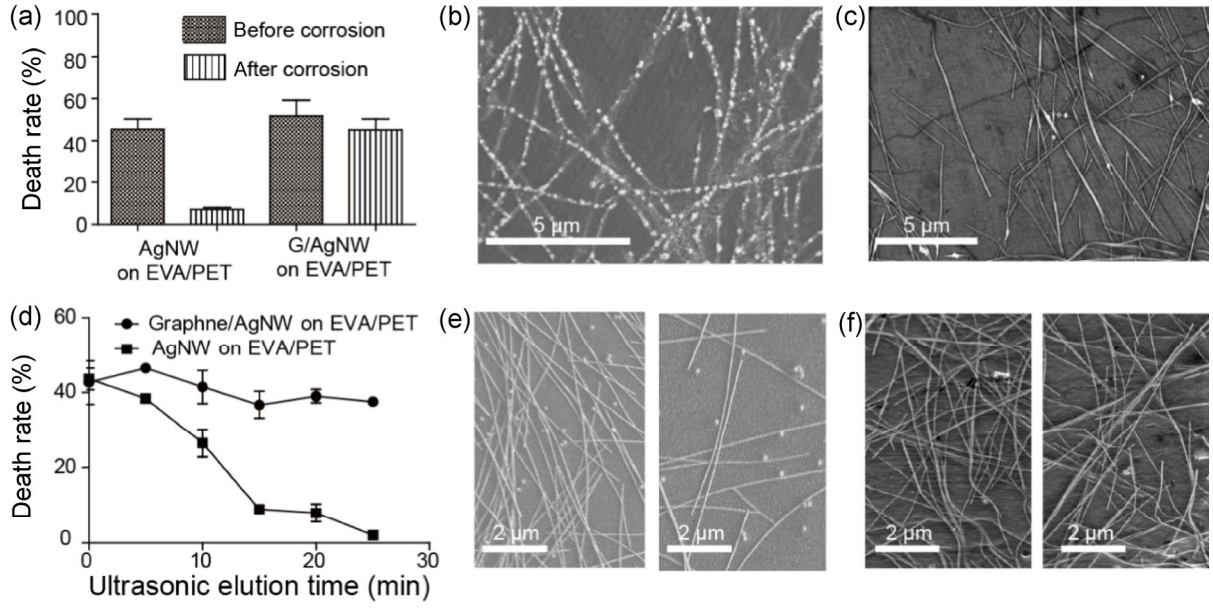

Figure 4 The robustness of the antimicrobial activity of the graphene/AgNW hybrid film against *C. albicans*. (a) Contrast of antimicrobial activity against *C. albicans* before and after aqueous Na_2S (4 wt.%) corrosion for a pure AgNW film and a graphene/AgNW hybrid film. (b) SEM image of a AgNW film immersed into Na_2S for 30 s, showing that the nanowires were corroded to break. (c) SEM image of graphene/AgNW film immersed into Na_2S for 2 min, showing that nanowires were still intact even after corrosion. (d) Contrast of antimicrobial activity before and after ultrasonic elution for the AgNW and graphene/AgNW films. (e) SEM image of AgNW film before (left) and after (right) ultrasonic elution for 10 min, showing the significant decrease in nanowire density. (f) SEM image of graphene/AgNW film before (left) and after (right) ultrasonic elution for 20 min, showing unchanged nanowire density.

Apart from the intrinsic antimicrobial activity, owing to the good electrical conductivity of the graphene/AgNW/EVA/PET film, as indicated in Fig. S5 in the ESM, the antimicrobial activity was expected to be enhanced by applying electrical input. Here, we demonstrated the increased antimicrobial activity by water electrolysis. The scheme is shown in Fig. 5(a). A graphene/AgNW/EVA/PET hybrid film with sheet resistance of ~20 Ω/□ was used as a cathode, a chemically inert electrode like platinum (Pt) wire as the cathode, and 1 mL of *C. albicans* SC5314 culture suspension as the electrolyte. Hydroxyl ions and hydrogen gas were generated at the surface of the hybrid film when a small voltage of ~5 V was applied with a current flow of ~3 mA. Note that such low voltage and small current flow do not harm human health. The generation of large amounts of hydroxyl ions allows the neutral microbial suspension (pH value at 7) to become strongly basic (pH value at 10), which is an unsuitable environment for many microorganisms. In order to investigate the antimicrobial strength of the graphene/AgNW/EVA/PET hybrid film under water electrolysis, the microorganisms were washed away from the surface of the graphene/AgNW/EVA/PET hybrid film with PBS in a sterilized Petri dish. Through serial 10-fold dilutions, 200 μL of each microbial suspension was spread on a Sabouraud Gentamicin Chloramphenicol (SGC) agar plate and incubated at 37 ℃ for 24 h. Surviving CFU count was performed afterwards. Figures 5(c)–5(e) show the number of fungi colonies grown on SGC plates as a function of the electrolysis time.

The photographs of the number of *Candida* cells on SGC agar plates clearly reflected the increased inhibition of microbial growth as a time function of water electrolysis. The antimicrobial efficiency could increase to nearly 100% in only 4 min under the above-mentioned electrolysis condition, as shown in Fig. 5(b), indicating that electrolysis might be an alternative way to enhance the antimicrobial activity through the conducting graphene/AgNW electrode.

Besides the antimicrobial transparent and conductive thin film, graphene/AgNW can be a versatile

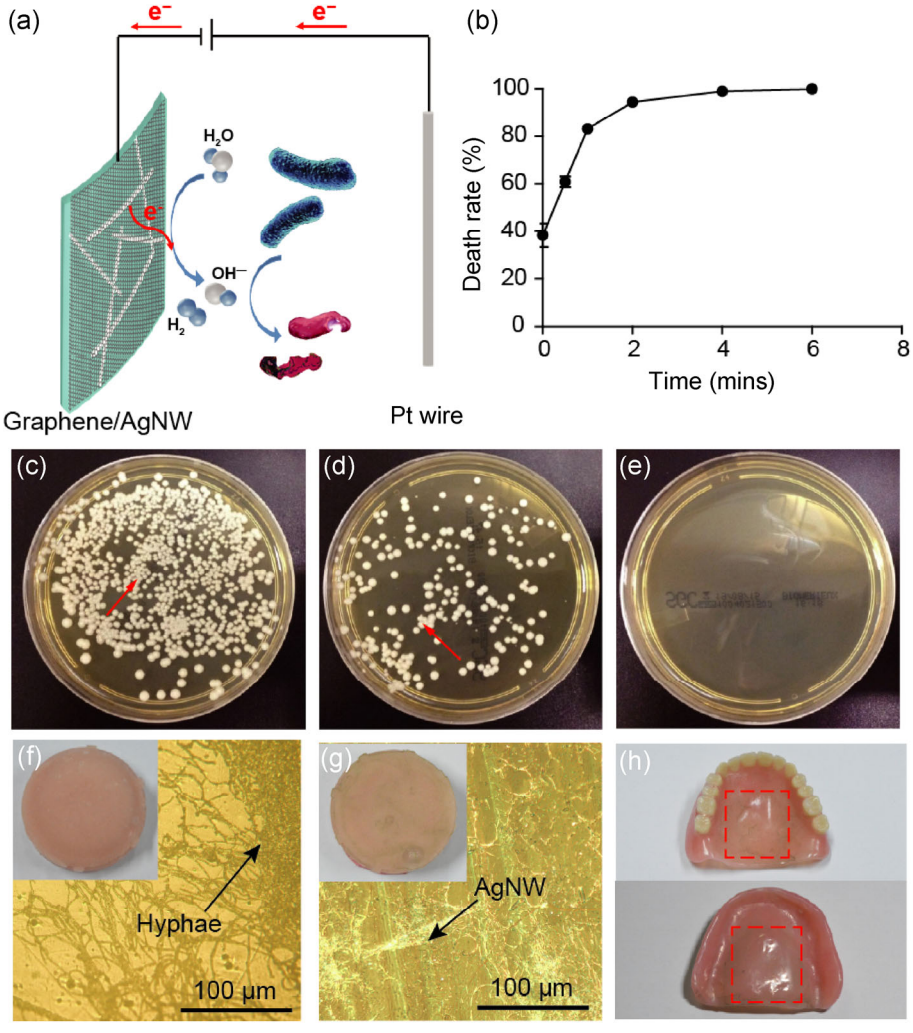

Figure 5 Enhanced antimicrobial activity against *C. albicans* by water electrolysis using a graphene/AgNW electrode. (a) Scheme of the enhanced antimicrobial activity by water electrolysis, where the graphene/AgNW hybrid film was used as the cathode and a Pt wire as the anode. (b) Death rate versus electrolysis time, showing that antimicrobial efficiency could be greatly enhanced by short-time electrolysis. (c)–(e) Representative photograph of CFU on SGC agar showing various electrolysis time points, i.e., (c) 0 s, (d) 30 s, and (e) 4 min. The light color indicates the cell colonies, whereas the darker areas shows agar without colonies. The red arrows show the cell colonies. (f) OM image of hyphae of *C. albicans* on the surface of a denture plate without graphene/AgNW coating, inset showing a photograph of the denture plate. (g) OM image of the surface of a denture plate with graphene/AgNW coating with 4-min electrolysis time, inset showing a photograph of the denture plate. (h) The photograph of a usable denture coated by graphene/AgNW. The dashed boxes show the graphene/AgNW coated areas.

antimicrobial coating to various medical devices such as prosthetics. In this work, a denture coated by graphene/AgNW was developed. The fabrication process is shown in the experimental section. The denture wearers usually suffer from stomatitis, which is the most common form of chronic oral inflammation and is mainly caused by the adherence and colonization by *C. albicans* [57]. The conductive graphene/AgNW coating not only enhanced the intrinsic antifungal ability of the denture, but also provided an efficient sterilization method by water electrolysis, as mentioned above. As shown in Fig. 5(f), *C. albicans* proliferated and formed hyphae on the surface of a denture plate without graphene/AgNW coating. Conversely, Fig. 5(g) shows that there were no fungi remaining on the surface of the denture plate with graphene/AgNW coating after only 4-min of electrolysis. In addition, a usable denture partially coated by graphene/AgNW

was developed and is shown in Fig. 5(h). Owing to the remarkable flexibility of graphene and AgNW, the coating process is compatible to the curved denture surface, sharing its application to various non-planar biomedical devices.

In conclusion, we report on the development of large-area CVD-grown monolayer graphene covered AgNWs with broad-spectrum and robust antimicrobial activity. The outer layer of the graphene film greatly reduced the microbial attachment. The robust and broad-spectrum antimicrobial activities against pathogenic Gram-negative (*E. coli*) and Gram-positive bacteria (*S. aureus*), and fungi (*C. albicans*) were mainly attributed to the sustained release of Ag^+ from underlying AgNWs, which was presumably originated from the electrochemical corrosion of silver. This graphene/AgNW coating maintained robust antimicrobial activity under tough environments due to the graphene coverage, capable of showing an antibacterial activity of up to 100% via the electrolysis of water using the conducting graphene/AgNW electrodes. A transparent and flexible antimicrobial cover, made of a graphene/AgNW/EVA/PET film, and an antimicrobial denture coated by graphene/AgNW were developed. This antimicrobial thin film coating with remarkable conductivity, transparency, and flexibility might be integrated into many functional electronic devices such as touchscreens and smart wearable healthcare devices, enabling safe uses and avoiding microbial threats.

Acknowledgements

This work was financially supported by the National Natural Science Foundation of China (Nos. 81000441, 21222303, and 21173004), the National Basic Research Program of China (Nos. 2014CB932500), and National Program for Support of Top-Notch Young Professionals.

Electronic Supplementary Material: Supplementary material (detailed experimental section, schematic of the fabrication process, surface morphology characterizations and so on) is available in the online version of this article at http://dx.doi.org/10.1007/s12274-016-0984-2.

References

[1] Irwansyah, I.; Li, Y. Q.; Shi, W. X.; Qi, D. P.; Leow, W. R.; Tang, M. B. Y.; Li, S. Z.; Chen, X. D. Gram-positive antimicrobial activity of amino acid-based hydrogels. *Adv. Mater.* **2015**, *27*, 648–654.

[2] Yang, C.; Ding, X.; Ono, R. J.; Lee, H.; Hsu, L. Y.; Tong, Y. W.; Hedrick, J.; Yang, Y. Y. Brush-like polycarbonates containing dopamine, cations, and PEG providing a broad-spectrum, antibacterial, and antifouling surface via one-step coating. *Adv. Mater.* **2014**, *26*, 7346–7351.

[3] Aviv, M.; Berdicevsky, I.; Zilberman, M. Gentamicin-loaded bioresorbable films for prevention of bacterial infections associated with orthopedic implants. *J. Biomed. Mater. Res. A* **2007**, *83*, 10–19.

[4] Gao, P.; Nie, X.; Zou, M. J.; Shi, Y. J.; Cheng, G. Recent advances in materials for extended-release antibiotic delivery system. *J. Antibiot.* **2011**, *64*, 625–634.

[5] Fischbach, M. A.; Walsh, C. T. Antibiotics for emerging pathogens. *Science* **2009**, *325*, 1089–1093.

[6] Huh, A. J.; Kwon, Y. J. "Nanoantibiotics": A new paradigm for treating infectious diseases using nanomaterials in the antibiotics resistant era. *J. Controlled Release* **2011**, *156*, 128–145.

[7] Zhu, C. L.; Yang, Q.; Liu, L. B.; Lv, F. T.; Li, S. Y.; Yang, G. Q.; Wang, S. Multifunctional cationic poly(p-phenylene vinylene) polyelectrolytes for selective recognition, imaging, and killing of bacteria over mammalian cells. *Adv. Mater.* **2011**, *23*, 4805–4810.

[8] Morones, J. R.; Elechiguerra, J. L.; Camacho, A.; Holt, K.; Kouri, J. B.; Ramírez, J. T.; Yacaman, M. J. The bactericidal effect of silver nanoparticles. *Nanotechnology* **2005**, *16*, 2346–2353.

[9] Kumar, A.; Vemula, P. K.; Ajayan, P. M.; John, G. Silver-nanoparticle-embedded antimicrobial paints based on vegetable oil. *Nat. Mater.***2008**, *7*, 236–241.

[10] Kvitek, L.; Panacek, A.; Soukupova, J.; Kolar, M.; Vecerova, R.; Prucek, R.; Holecova, M.; Zboril, R. Effect of surfactants and polymers on stability and antibacterial activity of silver nanoparticles (NPs). *J. Phys. Chem. C* **2008**, *112*, 5825–5834.

[11] Pal, S.; Tak, Y. K.; Song, J. M. Does the antibacterial activity of silver nanoparticles depend on the shape of the nanoparticle? A study of the Gram-negative bacterium *Escherichia coli*. *Appl. Environ. Microbiol.* **2007**, *73*, 1712–1720.

[12] Schoen, D. T.; Schoen, A. P.; Hu, L. B.; Kim, H. S.; Heilshorn, S. C.; Cui, Y. High speed water sterilization using one-dimensional nanostructures. *Nano Lett.* **2010**, *10*, 3628–3632.

[13] Nateghi, M. R.; Shateri-Khalilabad, M. Silver nanowire-functionalized cotton fabric. *Carbohydr. Polym.* **2015**, *117*, 160–168.

[14] Visnapuu, M.; Joost, U.; Juganson, K.; Künnis-Beres, K.; Kahru, A.; Kisand, V.; Ivask, A. Dissolution of silver nanowires and nanospheres dictates their toxicity to *Escherichia coli*. *BioMed Res. Int.* **2013**, *2013*, Article ID 819252.

[15] Tang, C. L.; Sun, W.; Lu, J. M.; Yan, W. Role of the anions in the hydrothermally formed silver nanowires and their antibacterial property. *J. Colloid Interface Sci.* **2014**, *416*, 86–94.

[16] Natalio, F.; André, R.; Hartog, A. F.; Stoll, B.; Jochum, K. P.; Wever, R.; Tremel, W. Vanadium pentoxide nanoparticles mimic vanadium haloperoxidases and thwart biofilm formation. *Nat. Nanotechnol.* **2012**, *7*, 530–535.

[17] Magrez, A.; Kasas, S.; Salicio, V.; Pasquier, N.; Seo, J. W.; Celio, M.; Catsicas, S.; Schwaller, B.; Forró, L. Cellular toxicity of carbon-based nanomaterials. *Nano Lett.* **2006**, *6*, 1121–1125.

[18] Schipper, M. L.; Nakayama-Ratchford, N.; Davis, C. R.; Kam, N. W. S.; Chu, P.; Liu, Z.; Sun, X. M.; Dai, H. J.; Gambhir, S. S. A pilot toxicology study of single-walled carbon nanotubes in a small sample of mice. *Nat. Nanotechnol.* **2008**, *3*, 216–221.

[19] Hu, W. B.; Peng, C.; Luo, W. J.; Lv, M.; Li, X. M.; Li, D.; Huang, Q.; Fan, C. H. Graphene-based antibacterial paper. *ACS Nano* **2010**, *4*, 4317–4323.

[20] Akhavan, O.; Ghaderi, E. Toxicity of graphene and graphene oxide nanowalls against bacteria. *ACS Nano* **2010**, *4*, 5731–5736.

[21] Liu, S. B.; Zeng, T. H.; Hofmann, M.; Burcombe, E.; Wei, J.; Jiang, R. R.; Kong, J.; Chen, Y. Antibacterial activity of graphite, graphite oxide, graphene oxide, and reduced graphene oxide: Membrane and oxidative stress. *ACS Nano* **2011**, *5*, 6971–6980.

[22] Tu, Y. S.; Lv, M.; Xiu, P.; Huynh, T.; Zhang, M.; Castelli, M.; Liu, Z. R.; Huang, Q.; Fan, C. H.; Fang, H. P. et al. Destructive extraction of phospholipids from *Escherichia coli* membranes by graphene nanosheets. *Nat. Nanotechnol.* **2013**, *8*, 594–601.

[23] Pham, V. T. H.; Truong, V. K.; Quinn, M. D. J.; Notley, S. M.; Guo, Y. C.; Baulin, V. A.; Kobaisi, M. A.; Crawford, R. J.; Ivanova, E. P. Graphene induces formation of pores that kill spherical and rod-shaped bacteria. *ACS Nano* **2015**, *9*, 8458–8467.

[24] LeOuay, B.; Stellacci, F. Antibacterial activity of silver nanoparticles: A surface science insight. *Nano Today* **2015**, *10*, 339–354.

[25] Lemire, J. A.; Harrison, J. J.; Turner, R. J. Antimicrobial activity of metals: Mechanisms, molecular targets and applications. *Nat. Rev. Microbiol.* **2013**, *11*, 371–384.

[26] Rizzello, L.; Pompa, P. P. Nanosilver-based antibacterial drugs and devices: Mechanisms, methodological drawbacks, and guidelines. *Chem. Soc. Rev.* **2014**, *43*, 1501–1518.

[27] Lok, C. N.; Ho, C. M.; Chen, R.; He, Q. Y.; Yu, W. Y.; Sun, H.; Tam, P. K. H.; Chiu, J. F.; Che, C. M. Silver nanoparticles: Partial oxidation and antibacterial activities. *J. Biol. Inorg. Chem.* **2007**, *12*, 527–534.

[28] Xiu, Z. M.; Zhang, Q. B.; Puppala, H. L.; Colvin, V. L.; Alvarez, P. J. J. Negligible particle-specific antibacterial activity of silver nanoparticles. *Nano Lett.* **2012**, *12*, 4271–4275.

[29] Reinsch, B. C.; Levard, C.; Li, Z.; Ma, R.; Wise, A.; Gregory, K. B.; Brown, G. E.; Lowry, G. V. Sulfidation of silver nanoparticles decreases *Escherichia coli* growth inhibition. *Environ. Sci. Technol.* **2012**, *46*, 6992–7000.

[30] Levard, C.; Mitra, S.; Yang, T.; Jew, A. D.; Badireddy, A. R.; Lowry, G. V.; Brown, G. E. Effect of chloride on the dissolution rate of silver nanoparticles and toxicity to *E. coli*. *Environ. Sci. Technol.* **2013**, *47*, 5738–5745.

[31] Xu, W. P.; Zhang, L. C.; Li, J. P.; Lu, Y.; Li, H. H.; Ma, Y. N.; Wang, W. D.; Yu, S. H. Facile synthesis of silver@graphene oxide nanocomposites and their enhanced antibacterial properties. *J. Mater. Chem.* **2011**, *21*, 4593–4597.

[32] Ma, J. Z.; Zhang, J. T.; Xiong, Z. G.; Yong, Y.; Zhao, X. S. Preparation, characterization and antibacterial properties of silver-modified graphene oxide. *J. Mater. Chem.* **2011**, *21*, 3350–3352.

[33] Kholmanov, I. N.; Stoller, M. D.; Edgeworth, J.; Lee, W. H.; Li, H. F.; Lee, J. H.; Barnhart, C.; Potts, J. R.; Piner, R.; Akinwande, D. et al. Nanostructured hybrid transparent conductive films with antibacterial properties. *ACS Nano* **2012**, *6*, 5157–5163.

[34] Li, C.; Wang, X. S.; Chen, F.; Zhang, C. L.; Zhi, X.; Wang, K.; Cui, D. X. The antifungal activity of graphene oxide-silver nanocomposites. *Biomaterials* **2013**, *34*, 3882–3890.

[35] Li, J. H.; Wang, G.; Zhu, H. Q.; Zhang, M.; Zheng, X. H.; Di, Z. F.; Liu, X. Y.; Wang, X. Antibacterial activity of large-area monolayer graphene film manipulated by charge transfer. *Sci. Rep.* **2014**, *4*, 4359.

[36] Dellieu, L.; Lawarée, E.; Reckinger, N.; Didembourg, C.; Letesson, J. J.; Sarrazin, M.; Deparis, O.; Matroule, J. Y.; Deparis, J. F. Do CVD grown graphene films have antibacterial activity on metallic substrates? *Carbon* **2015**, *84*, 310–316.

[37] Chen, R. Y.; Das, S. R.; Jeong, C.; Khan, M. R.; Janes, D. B.; Alam, M. A. Co-percolating graphene-wrapped silver nanowire network for high performance, highly stable, transparent conducting electrodes. *Adv. Funct. Mater.* **2013**, *23*, 5150–5158.

[38] Lee, M. S.; Lee, K.; Kim, S. Y.; Lee, H.; Park, J.; Choi, K. H.; Kim, H. K.; Kim, D. G.; Lee, D. Y.; Nam, S. et al. High-performance, transparent, and stretchable electrodes using graphene-metal nanowire hybrid structures. *Nano Lett.* **2013**, *13*, 2814–2821.

[39] Deng, B.; Hsu, P. C.; Chen, G. C.; Chandrashekar, B. N.; Liao, L.; Ayitimuda, Z.; Wu, J. X.; Guo, Y. F.; Lin, L.; Zhou, Y. et al. Roll-to-roll encapsulation of metal nanowires between graphene and plastic substrate for high-performance flexible transparent electrodes. *Nano Lett.* **2015**, *15*, 4206–4213.

[40] Lee, G. H.; Cooper, R. C.; An, S. J.; Lee, S.; van der Zande, A.; Petrone, N.; Hammerherg, A. G.; Lee, C.; Crawford, B.; Oliver, W. et al. High-strength chemical-vapor deposited graphene and grain boundaries. *Science* **2013**, *340*, 1073–1076.

[41] O'Hern, S. C.; Stewart, C. A.; Boutilier, M. S. H.; Idrobo, J. C.; Bhaviripudi, S.; Das, S. K.; Kong, J.; Laoui, T.; Atieh, M.; Karnik, R. Selective molecular transport through intrinsic defects in a single layer of CVD graphene. *ACS Nano* **2012**, *6*, 10130–10138.

[42] Tao, A.; Kim, F.; Hess, C.; Goldberger, J.; He, R. R.; Sun, Y. G.; Xia, Y. N.; Yang, P. D. Langmuir-Blodgett silver nanowire monolayers for molecular sensing using surface-enhanced Raman spectroscopy. *Nano Lett.* **2003**, *3*, 1229–1233.

[43] An, Y. H.; Friedman, R. J. Concise review of mechanisms of bacterial adhesion to biomaterial surfaces. *J. Biomed. Mater. Res.* **1998**, *43*, 338–348.

[44] Mcallister, E. W.; Carey, L. C.; Brady, P. G.; Heller, R.; Kovacs, S. G. The role of polymeric surface smoothness of biliary stents in bacterial adherence, biofilm deposition, and stent occlusion. *Gastrointest. Endosc.* **1993**, *39*, 422–425.

[45] Quirynen, M.; van der Mei, H. C.; Bollen, C. M. L.; Schotte, A.; Marechal, M.; Doornbusch, G. I.; Naert, I.; Busscher, H. J.; van Steenberghe, D. An *in vivo* study of the influence of the surface roughness of implants on the microbiology of supra- and subgingival plaque. *J. Dent. Res.* **1993**, *72*, 1304–1309.

[46] Hogt, A. H.; Dankert, J.; DeVries, J. A.; Feijen, J. Adhesion of coagulase-negative staphylococci to biomaterials. *J. Gen. Microbiol.* **1983**, *129*, 2959–2968.

[47] Ludwicka, A.; Jansen, B.; Wadström, T.; Pulverer, G. Attachment of staphylococci to various syntheticpolymers. *Zentralbl. Bakteriol. Mikrobiol. Hyg. A* **1984**, *256*, 479–489.

[48] Geim, A. K.; Novoselov, K. S. The rise of graphene. *Nat. Mater.* **2007**, *6*, 183–191.

[49] Taherian, F.; Marcon, V.; van der Vegt, N. F. A.; Leroy, F. What is the contact angle of water on graphene? *Langmuir* **2013**, *29*, 1457–1465.

[50] Schriver, M.; Regan, W.; Gannett, W. J.; Zaniewski, A. M.; Crommie, M. F.; Zettl, A. Graphene as a long-term metal oxidation barrier: Worse than nothing. *ACS Nano* **2013**, *7*, 5763–5768.

[51] Shao, Y. Y.; Wang, J.; Wu, H.; Liu, J.; Aksay, I. A.; Lin, Y. H. Graphene based electrochemical sensors and biosensors: A review. *Electroanalysis* **2010**, *22*, 1027–1036.

[52] Zhou, M.; Zhai, Y. M.; Dong, S. J. Electrochemical sensing and biosensing platform based on chemically reduced graphene oxide. *Anal. Chem.* **2009**, *81*, 5603–5613.

[53] Li, P.; Zhou, C. C.; Rayatpisheh, S.; Ye, K.; Poon, Y. F.; Hammond, P. T.; Duan, H. W.; Chan-Park, M. B. Cationic peptidopolysaccharides show excellent broad-spectrum antimicrobial activities and high selectivity. *Adv. Mater.* **2012**, *24*, 4130–4137.

[54] Kholmanov, I. N.; Magnuson, C. W.; Aliev, A. E.; Li, H. F.; Zhang, B.; Suk, J. W.; Zhang, L. L.; Peng, E.; Mousavi, S. H.; Khanikaev, A. B. et al. Improved electrical conductivity of graphene films integrated with metal nanowires. *Nano Lett.* **2012**, *12*, 5679–5683.

[55] Lv, M.; Su, S.; He, Y.; Huang, Q.; Hu, W. B.; Li, D.; Fan, C. H.; Lee, S. T. Long-term antimicrobial effect of silicon nanowires decorated with silver nanoparticles. *Adv. Mater.* **2010**, *22*, 5463–5467.

[56] Christensen, F. M.; Johnston, H. J.; Stone, V.; Aitken, R. J.; Hankin, S.; Peters, S.; Aschberger, K. Nano-silver-feasibility and challenges for human health risk assessment based on open literature. *Nanotoxicology* **2010**, *4*, 284–295.

[57] Bakhshi, M.; Taheri, J. B.; Shabestari, S. B.; Tanik, A.; Pahlevan, R. Comparison of therapeutic effect of aqueous extract of garlic and nystatin mouthwash in denture stomatitis. *Gerodontology* **2012**, *29*, e680–e684.